A NEW DIMENSION TO LUNAR MAGMATISM: NEW INTERPRETATIONS OF APOLLO BASALT PETROGENESIS FROM X-RAY COMPUTED TOMOGRAPHY. A. J. Gawronska[1], C. L. McLeod[1], E. H. Blumenfeld[2], R. Hanna[3], R. A. Zeigler[4]. [1]Dept. Of Geology & Envt. Earth Science, Miami University, Oxford OH, 45056. (gawronaj@miamioh.edu). [2]LZ Technology, JETS Contract, NASA JSC, Houston TX, 77058, [3]Jackson School of Geosciences, University of Texas at Austin, Austin TX, 78712. [4]NASA JSC, Houston TX, 77058.

Introduction: Lunar basaltic samples returned in the 1960's and 1970's through the Apollo missions have provided unparalleled insights into the processes associated with extraterrestrial magmatism and volcanism. Numerous studies undertaken on these samples have documented the textural (e.g., glassy to microgabbroic) and geochemical (exemplified by characteristic Ti, K, and Al content) diversity that exists in these samples [e.g., 1-2].

However, geologic samples have been traditionally studied in two dimensions (2D) via interrogation of thin sections and subsequent *in-situ* chemical analyses. Yet the returned Apollo samples are three-dimensional (3D) rocks and preserve evidence of lunar magmatic and volcanic processes in 3D. Considering the relative paucity of lunar samples when compared to terrestrial samples, sample destruction via traditional methods like sectioning and dissolving does not support sample preservation long-term. Thus, the non-destructive technique of X-ray computed tomography (XCT) was applied in this study to 1) compare quantitative mineralogies to 2D datasets (from thin section studies), 2) evaluate magmatic petrogeneses on the Moon, and 3) demonstrate the role of XCT in scientific studies and curation of extraterrestrial materials.

Methods: Six Apollo basalts were scanned: 10057,19 (fine-grained, high-K ilmenite), 12038,7 (coarse-grained, feldspathic), 12043,0 (medium-grained, pigeonite), 15085,0 (coarse-grained, pigeonite), 15556,0 (vesicular, olivine-normative) 70017,8 (medium-grained, low-K ilmenite). For further details on XCT methodology see [3-6]. *Dragonfly* [7] and *ImageJ* [8] were used to adjust scan brightness and contrast values, then *Blob3D* [9] was used to segment and separate components and extract particle dimensions and orientations. In order to evaluate cooling histories, we developed an Excel spreadsheet to automatically quantify particle size distribution (PSD) profiles. In order to interpret stress imparted on and recorded by a magma upon emplacement, the extracted orientation data was plotted on lower hemisphere projections using *Stereo32* [10].

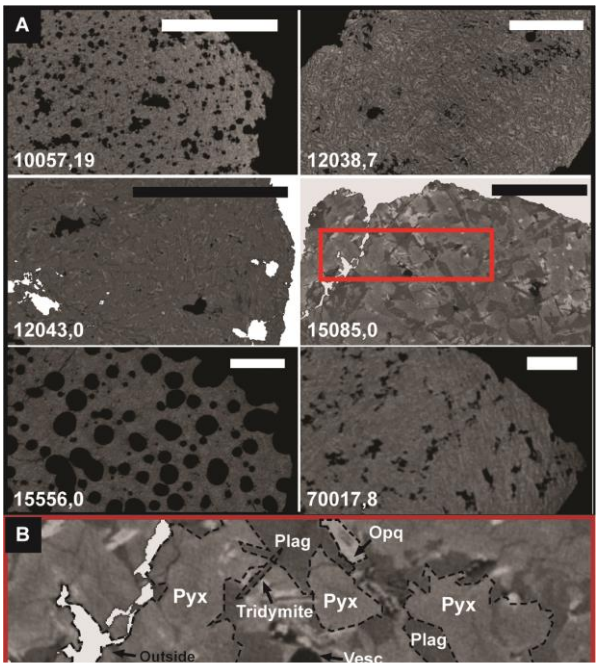

Fig. 1: A) Scan slices for each of the samples studied here. Scale bars 10 mm. B) Detail of sample 15085,0 scan slice showing sample components.

Results: Based on XCT data, plagioclase feldspar and pyroxene form interconnected networks (Fig. 1); it was therefore only possible to extract individual particle data on minor sample components (Table 1), like vesicles and opaques (ilmenite, Fe-rich spinel). Based on kinks in opaque PSD profiles (Fig. 2), and a kinked vesicle PSD for 15556,0, all samples except 12043,0 are interpreted to have experienced a change in cooling environment, whereas sample 12038,7 may have experienced crystal accumulation based on its concave up profile [11]. With respect to orientations (Fig. 3), neither the opaque particles nor vesicles appear to record any statistically significant orientation ($C<0$, [12]). However, the samples with highest clustering visually (10057,19, 70017,8) also have the highest C values, and thus may preserve some minimal stress due to flow, even though this is not statistically significant. Through XCT, it was also possible to quantify sample vesicularity. It is interpreted here that samples 10057,19 (9.7% vesicles) and 15556,0 (48.0% vesi-

cles) represent the initial stages of an eruption as volatile species exsolve, in contrast to the remaining samples [13].

Discussion: Volumetric mineralogies reported here generally match modal mineralogies reported in prior 2D thin section studies. For all samples, energy of X-rays during the scans was relatively high (~170 to 450) in order to penetrate the samples, but such high energy X-rays are less sensitive to changes in sample density and chemistry [14]; this appears to have made sample components less distinct and more challenging to separate. Thus, it is recommended that future studies scan smaller sample chips at lower X-ray energies [6]. For all samples studied here, application of XCT has provided a greater depth of knowledge regarding conditions experienced by the magma during eruption and emplacement. As humanity looks forward to examine returned samples from Chang'e-5, Hayabusa 2, and future asteroid sample return alongside crewed missions to the Moon, Mars, and beyond, it is recommended that all materials are initially characterized via nondestructive XCT methods. XCT is a crucial asset to sample curation, sample preservation, and the future of planetary exploration.

Acknowledgments: These XCT image data were produced by Astromaterials 3D at the High-Resolution X-ray Computed Tomography Facility of the University of Texas at Austin (UTCT) for NASA's Acquisition & Curation Office; Astromaterials 3D was funded by NASA Planetary Data Archiving, Restoration, and Tools Program, Proposal No.: 15-PDART15_2-0041.

References:

[1] Meyer et al. (2016) The Lunar Sample Compendium. [2] Neal C. R. and Taylor L. A. (1992) *GCA 56*, 2177–2211. [3] Ebel D. S. and Rivers M. L. (2007) *Meteorit. Planet. Sci. 42*, 1627-1646. [4] Jerram D. A. and Higgins M. D. (2007) *Elements 3(4)*, 239-245. [5] Cnudde V. and Boone M. N. (2013) *Earth Sci. Rev. 123*, 1-17. [6] Hanna R. D. and Ketcham R. A. (2017) *Chem. Erde 77*, p. 547-572. [7] Object Research Inc. (2016) www.theobjects.com/dragonfly. [8] Schneider C. A. et al. (2012) *Nat.Methods 9*(7), 671-675. [9] Ketcham R. A. (2005) *Geosphere 1*(1), 32-41. [10] Roeller K. and Trepmann C. (2010) *Stereo32* [11] Neal C. R. et al. (2015) *GSA 148*, 62-80. [12] Woodcock N. H. and Naylor M. A. (1983) *J. Struct. Geol. 5*, 539–548. [13] Wilson L. and Head J. W. (1981) *JGR 86*, 2971-3001 [14] Ketcham R. and Carlson W. D. (2001) *Comput. Geosci. 24*(7), 381-400.

TABLE 1. SUMMARY OF SAMPLE MINERALOGY

Sample Number	Opaques†		Pyroxene		Plagioclase feldspar		Total rock volume (mm^3)
	Here (vol. %)	Other studies*	Here (vol. %)	Other studies*	Here (vol. %)	Other studies*	
10057,19	19.8	15.5-15.7	49.3	50.8-50.9	30.8	19.2-24	38237
12038,7	2.7	3.46-10	63.5	48.8-55	33.8	30-44	101434
12043,0	1.2	3.5	76.9	57.7	21.8	32.9	16380
15085,0	4.9	3-3.5	62.5	40-66	29.5	22-60	74390
15556,0	1.2	3-8	38.3	50-57	60.5	30-38	180768
70017,8	4.7	19.2-22.8	48.2	49.3-57.6	45.4	19.8-26	333627

*Data gathered from the Lunar Sample Compendium (Meyer, 2016).

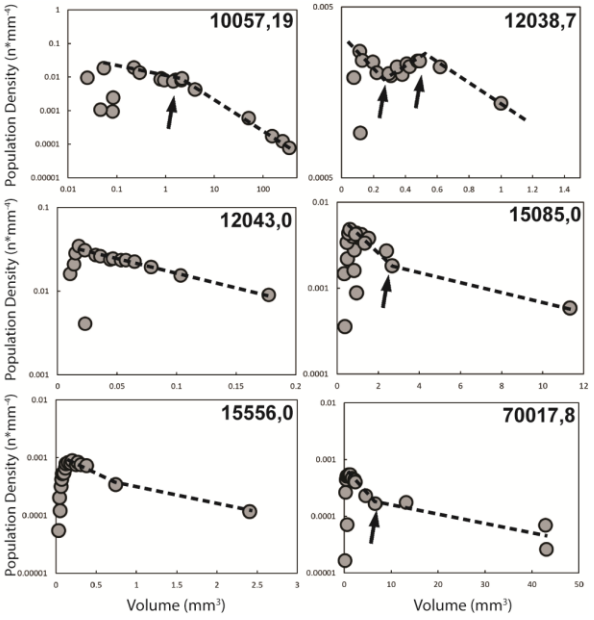

Fig. 2: Particle size distributions (PSDs) for opaque phases. Dashed lines represent lines of best fit, arrows indicate apparent "kinks" which suggest a change in cooling environment.

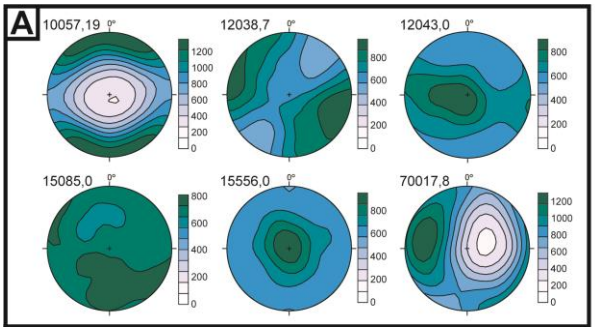

Fig. 3: Stereonets of distribution of opaque long axis orientations. All stereonets are lower-hemisphere projections.